forests

MDPI

Article

Changes in Gross Primary Production in Response to Afforestation in the Hilly Loess Plateau of Northern Shaanxi, China

Wangjun Li and Dechao Chen *

School of Geography Science and Geomatics Engineering, Suzhou University of Science and Technology, Suzhou 215009, China
* Correspondence: dcchen@mail.usts.edu.cn

Abstract: As a large-scale afforestation initiative, the Grain for Green (GFG) program was implemented for more than decade in the hilly Loess Plateau of Northern Shaanxi starting in 1999 and inevitably affected plant biomass production. This study evaluated the trend and magnitude of gross primary production (GPP) changes with VPM in the study area over 2000–2012 and quantitatively identified GFG's contribution. The results indicate that the regional mean GPP was 529.6 to 854.7 g C m^{-2} yr^{-1}, which significantly increased by 1.63% per year during the period. At the pixel level, 80% of the pixels presented an increasing trend in annual GPP, and in nearly half of the region, the increasing trend was statistically significant. Spatial analyses showed that the GPP increased more significantly in the gully areas of the middle north area, while no evident change trend was observed in the southern forestland areas. Statistical data from relevant yearbooks and interpreted data from high-resolution images show that the GFG program promoted vegetation restoration. Taking the increased area of forestland to indicate the achievements of GFG, we estimated, using regression analyses, that the afforestation contributed 40%–60% to the increased GPP in the region during 2000–2012. Overall, the ecosystem had a positive response to the Grain for Green (GFG) program in Northern Shaanxi.

Keywords: Grain for Green program; GPP; VPM; change trend; the Loess Plateau

check for updates

Citation: Li, W.; Chen, D. Changes in Gross Primary Production in Response to Afforestation in the Hilly Loess Plateau of Northern Shaanxi, China. *Forests* **2022**, *13*, 1414. https://doi.org/10.3390/f13091414

Academic Editor: Mark S. Ashton

Received: 11 August 2022
Accepted: 31 August 2022
Published: 2 September 2022

Publisher's Note: MDPI stays neutral with regard to jurisdictional claims in published maps and institutional affiliations.

Copyright: © 2022 by the authors. Licensee MDPI, Basel, Switzerland. This article is an open access article distributed under the terms and conditions of the Creative Commons Attribution (CC BY) license (https://creativecommons.org/licenses/by/4.0/).

1. Introduction

Northern Shaanxi is located in the north center of the Loess Plateau, with a semiarid to subhumid climate and a vulnerable ecosystem. This region is sensitive to global changes and was heavily affected by human activities during past decades. Due to overcultivation of the sloping lands, the region suffered from serious soil erosion. To alleviate this land degradation problem, the Chinese government implemented the Grain for Green (GFG) program in 1999 by supplying grain or money as a subsidy to help farmers convert sloping farmlands into forestland/grassland, plant trees on degraded land, and reduce grazing on grassland. Many studies indicated that this program has stimulated a positive change in vegetation [1–4], land use/land cover [5], soil erosion [6,7], and carbon sequestration [8,9]. This program has also yielded obvious changes in crop production [10,11] and farmer household livelihoods [12,13]. The impact of GFG has had strong support in Northern Shaanxi [14]. One of the most important results of GFG is the promotion of vegetation, which can improve soil erosion in this area. Thus, in order to determine the response of the ecosystem to GFG, it is critical to find the changes in vegetation, including the quantity and, especially, the quality. Gross primary productivity (GPP) is the rate of carbon fixation or gross assimilation per unit of ground surface area [15] and is a measure of photosynthesis representing the primary conduit of carbon flux from the atmosphere to the land [16]. GPP changes can represent the activity of the vegetation to some extent, so such changes provide a good indicator to determine variation in vegetation quality.

With progress in remote sensing technology, it has become common practice to utilize imagery data to estimate GPP at large scales [17]. Many models have been developed for this purpose, including CASA [18], GLO-PEM [19], C-Fix [20], MODIS-PSN [21], VPM [22], EC-LUE [23], TG [24], and VI [25]. Of these models, the eco-process model CASA is more widely used than others but remains constrained by difficulties in obtaining data for the complex driving variables [26,27]. In contrast, the vegetation photosynthesis model (VPM) developed by Xiao et al. [22] has the lowest requirements for observational data. This model uses an improved EVI (enhanced vegetation index) to estimate the absorbed fraction of photosynthetically active radiation via green (photosynthetically active) vegetation and LSWI (land surface water index) to estimate water stress on light use efficiency. This model has been applied to estimate the GPPs of various vegetation types, including forests, grasslands, and maize crops and has been validated using CO_2 flux tower data [28–30] in several areas, including northern China.

The aim of this study is to quantitatively identify the magnitude of GPP changes and GFG contributions, taking the hilly region of Northern Shaanxi as a case area. With this aim, the annual GPP was first estimated for 2000 to 2012 using the VPM model with MODIS imagery and climate data; then, the change trend and magnitude were detected using a Mann–Kendall test and Sen's slope estimator. Finally, the contribution of GFG to GPP variation was determined using linear regressions. In this way, we determined the response of the ecosystem to GFG in Northern Shaanxi.

2. Study Area and Data Acquisition

2.1. Site Description

The study region of northern Shaanxi Province [36°9′ N–39°35′ N, 107°14′ E–111°16′ E] (Figure 1) has an area of 8.4 M ha, covering 25 county-level administrative units. This is a typical and highly dissected hilly region dominated by slope land with an altitude of 385–1911 m. The mean annual temperature is 8.2–13.1 °C and increases from north to south. The mean annual precipitation is around 600 mm in the southeast and gradually decreases to below 400 mm in the northwest. The precipitation varies seasonally, with more than 60% falling in the rainy season of July to September. Precipitation also varies significantly from year to year, with relative variation (CV) of 20%–30% [31]. In 2000, the land cover mainly featured cropland (52%), grassland (26%), forestland (11%), and shrubland (11%).

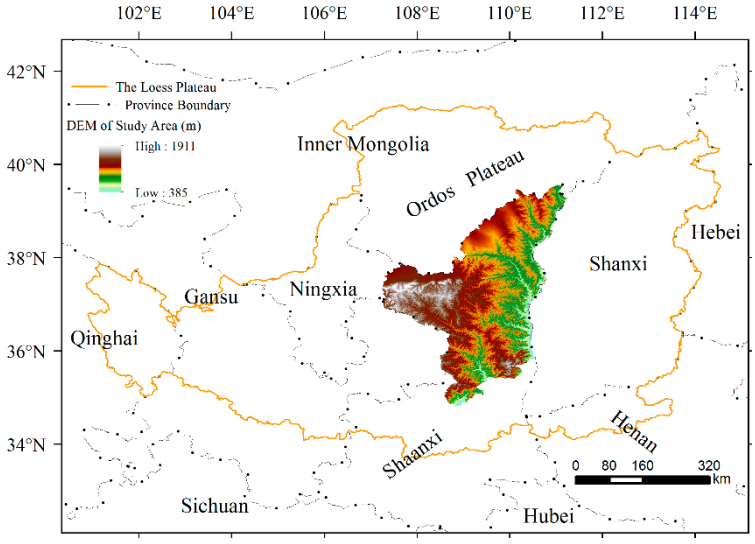

Figure 1. The location of the study area.

2.2. MODIS Data and Calculation of Vegetation Indices

MODIS Land Products MOD09A1 for the years of 2000 to 2012 was downloaded from NASA (http://ladsweb.nascom.nasa.gov/data/search.html, accessed on 26 June 2017).

The dataset features 7 spectral bands in HDF format at a spatial resolution of 500 m, a time resolution of 8 days, and corrections for atmospheric, aerosol scattering, and cloudiness. In this study, 5 spectral bands were used to generate the spatial dataset for visible albedo (VA), enhanced vegetation index (EVI), and land surface water index (LSWI) with the equations [32] below:

$$VA = 0.331 \cdot \rho_{red} + 0.0424 \cdot \rho_{blue} + 0.0246 \cdot \rho_{green} \quad (1)$$

$$EVI = \frac{2.5 \cdot (\rho_{nir} - \rho_{red})}{\rho_{nir} + (6 \cdot \rho_{red} - 7.5 \cdot \rho_{blue}) + 1} \quad (2)$$

$$LSWI = \frac{\rho_{nir} - \rho_{swir}}{\rho_{nir} + \rho_{swir}} \quad (3)$$

where ρ_{red}, ρ_{blue}, ρ_{nir}, ρ_{green}, and ρ_{swir} are the reflectance of the red (620–670 nm), blue (459–479 nm), near-infrared (841–876 nm), green (545–565 nm), and shortwave infrared (1628–1652 nm) bands, respectively.

2.3. MODIS Data and Calculation of Vegetation Indices

Daily precipitation, temperature, sunshine duration, wind speed, and relative humidity were obtained from the China Meteorological Data Sharing Service System (http://cdc.cma.gov.cn, accessed on 12 November 2016) for the years of 2000 to 2012 at 17 meteorological stations in and surrounding the region. Daily solar radiation data were not available and were instead estimated with the Angstrom equation [33,34], $R_a = R_s \cdot (a + b \cdot n/N)$, where R_a and R_s are the terrestrial surface and extraterrestrial radiation, and n and N are the observed and maximum possible daily sunshine duration, respectively. The coefficients *a* and *b* were set to 0.18 and 0.55, respectively, as suggested by Li et al. for the Loess Plateau [35]. Photosynthetically active radiation (PAR) was considered as half of the total radiation [18], and the units were converted to mol m^{-2} using the conversion coefficient of 4.57 μmol J^{-1} [36].

To match the time and spatial resolution of the MOD09A1 data, time series data representing the mean temperature and total PAR for each 8-day period were prepared year-by-year for 2000 to 2012, based on daily records from the 17 meteorological stations. Then, the data were interpolated sequentially to obtain the values for each grid at a size of 500 × 500 m using the ordinary kriging approach.

2.4. Vegetation and Land Use Change Data

Based on China's Vegetation Map (1:1,000,000) [37] published in 2001, the spatial vegetation data for the study region were extracted and regrouped into four land use types: cropland, forestland, grassland, and shrubland (Figure 2). This map, which presents the general land use condition in the starting year of the study period, was used as the basis to analyze the results.

Two types of land use change data were collected: statistical data for the annual afforestation area during 2000–2012 from local yearbooks and data obtained by interpreting high-resolution images for a typical hilly area of 900 km^2 (30 × 30 km, 36°45′15″–37°1′26″ N, and 109°25′2″–109°45′22″ E) in the middle area of the region (Figure 2). Two available 2.5 m resolution images (i.e., the SPOT image on 9 June 2003 and the ALOS image on 9 September 2009) were obtained to delineate land use types in 2003 and 2009 via visual interpretation. These two land use maps were then overlapped to extract the area change for each land use type between 2009 and 2003.

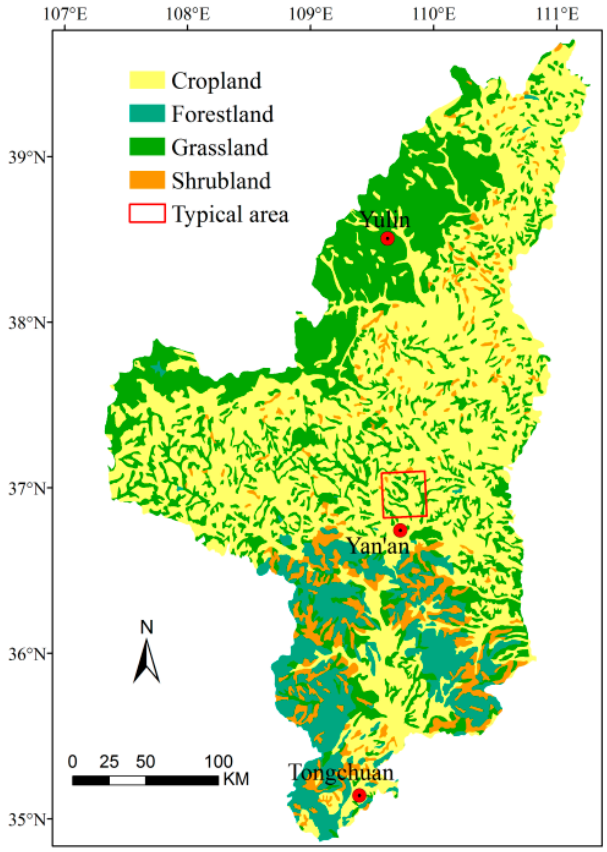

Figure 2. Spatial distributions of major land use types in Northern Shaanxi for 2000.

3. Methods

The analysis was conducted in three steps. The annual GPP was first estimated for 2000 to 2012. followed by detection of the GPP trend and change rate. Finally, linear regressions were applied to identify GFG's contribution to GPP changes.

3.1. Estimation of Gross Primary Production

The vegetation photosynthesis model (VPM) was used to estimate GPP, as follows [22]:

$$GPP = \varepsilon_g \cdot FAPAR \cdot PAR \quad (4)$$

$$\varepsilon_g = \varepsilon_{max} \cdot T_{scalar} \cdot W_{scalar} \cdot P_{scalar} \quad (5)$$

where ε_g (ε_{max}) is the actual (maximum) plant light use efficiency (g C mol^{-1} PAR); PAR is the photosynthetically active radiation (mol m^{-2} (8d)$^{-1}$), and FAPAR is the absorbed fraction of PAR, set equal to EVI [22] but not exceeding 0.95 based on Potter et al. [14]. T_{scalar}, $W_{scalar,}$ and P_{scalar} are the stress scalar values ranging from 0 to 1, which are used here to account for the effect of temperature, water, and leaf age, respectively, on light use efficiency.

The ε_{max} value was estimated at a time step of 8 days for each pixel via the empirical equation developed by Wang et al. [38] using eddy covariance data in northern China. To derive the ε_{max} value at the pixel level, this equation was based on two parameters, the maximum EVI (EVI_{max}) and minimum visible albedo (VA_{min}) within the growing season, as presented below:

$$\varepsilon_{max} = \exp(1.428 \cdot EVI_{max} - 6.295 \cdot VA_{min} - 1.211). \quad (6)$$

The temperature scalar (T_{scalar}) was calculated using the algorithm of the CASA model [18], and W_{scalar} and P_{scalar} were computed using the VPM equations [22]:

$$T_{\text{scalar}} = \frac{1.1814 \cdot \left(0.8 + 0.02 \cdot T_{opt} - 0.0005 \cdot T_{opt}^2\right)}{\left(1 + \exp\left(0.3 \cdot \left(T - T_{opt} - 10\right)\right)\right) \cdot \left(1 + \exp\left(0.2 \cdot \left(T_{opt} - T - 10\right)\right)\right)} \quad (7)$$

$$W_{\text{scalar}} = \frac{1 + \text{LSWI}}{1 + \text{LSWI}_{\text{max}}} \quad (8)$$

$$P_{\text{scalar}} = \frac{1 + \text{LSWI}}{2} \quad (9)$$

where T is the 8-day mean air temperature, and T_{opt} is the optimum temperature for a specific plant type. Here, T_{scalar} is set to 0 when T is lower than 0 °C. T_{opt} is set equal to the mean temperature at which the mean EVI value over the 13 years of 2000–2012 reaches its maximum based on previous studies [18,19]. LSWI_{max} is the maximum LSWI within the plant growing season for individual pixels. From the 13-year LSWI data, we selected the maximum value within the photosynthetically active period as an estimate of LSWI_{max}. P_{scalar} was set to 1 for grass during the whole growing season. For the other three vegetation types, P_{scalar} was estimated using Equation (9) from bud burst to leaf expansion and from leaf falling to wilting; the value was set to 1 during the full expansion period between mid-May and the end of August, as determined from the EVI curve.

3.2. Detection of Trend and Change Rate in GPP

The Mann–Kendall (MK) test [39] and Sen's slope estimator [40] were combined to detect the trend and change amplitude of annual GPP from 2000 to 2012. MK uses the normal approximation Z test to determine whether time series data have an upward (positive Z) or downward (negative Z) trend. At a σ level of significance, a significant trend was considered to be present if the absolute Z value was greater than $Z_{1-\sigma/2}$, where $Z_{1-\sigma/2}$ was obtained from the standard normal cumulative distribution tables [41]. Then, the slope value Q, i.e., the change rate per time unit, was estimated using Sen's method. In this study, we developed a program using the MATLAB software to calculate the Z test value and Q value of annual GPP at pixel and regional levels. The Q value indicates the mean annual change rate of GPP, which was presented as a percentage of the 13-year average GPP.

3.3. Detection of Ecorestoration Effects on GPP

The major aim of the GFG program was to rehabilitate destroyed vegetation by converting sloping farmland into forestland and planting trees on degraded grassland. Therefore, changes in forestland area were selected to determine program achievements and used as an indicator to identify the contribution of such changes to changes in GPP via regression analyses, in order to calculate the correlation coefficient R^2 between changes in GPP and forestland area. For the whole region, we used county as the spatial unit and selected the mean annual change rates in GPP and forestland area during 2000–2012 as variables. For each county, the annual change rate of GPP was estimated using Sen's slope method, and the annual forestland change rate was based on statistical data of the afforestation area, expressed as a percentage of the mean annually afforested area to the total county area. For a typical area, we divided the region into 117 fishnet areas (3 × 3 km) and obtained changes in the GPP and forestland area between 2003 and 2009 in each fishnet using ArcGIS. Then, the 117 datasets were regressed to obtain the correlation coefficient.

GPP changes can also be affected by climatic variation. To identify the effects of such changes, we selected the aridity index (K), the ratio of annual precipitation to potential evapotranspiration [31], as an integrated indicator. The relationship between changes in GPP and K values was then examined at three representative sites of Luochuan (35°49′ N, 109°30′ E), Suide (37°30′ N, 110°13′ E), and Yulin (38°16′ N, 109°47′ E), where the main land use is forestland, cropland, and grassland, respectively. A window area of 3 × 3 pixels surrounding each of these three meteorological stations was selected, and the mean GPP

was extracted for each year during 2000–2012 using ArcGIS. With yearly data for the GPP and K values, the changes between each year and the previous year were obtained and then linearly regressed to assess the presence of a significant correlation.

4. Results

4.1. Spatial Variation of GPP

The mean annual GPP during 2000–2012 at the pixel level was 1.7 to 3185.5 g C m^{-2} and roughly decreased from south to north (Figure 3) alongside changes in the vegetation and climate conditions. In the drier northern grassland areas, the mean GPP was generally below 460 g C m^{-2} yr^{-1} and significantly lower than that in the southern forestland areas, where the mean GPP was normally above 1350 g C m^{-2} yr^{-1}. In the middle area, where the land use mainly includes cropland, the mean GPP was mostly 460–840 g C m^{-2} yr^{-1}. Statistical results indicate that the mean GPP in 99% of the region was between 150 and 2500 g C m^{-2} yr^{-1}, with a regional average of 720 g C m^{-2} yr^{-1}. For the four land use areas of grassland, cropland, shrubland, and forestland, the mean GPP was 472, 558, 1215, and 1602 g C m^{-2} yr^{-1}, respectively.

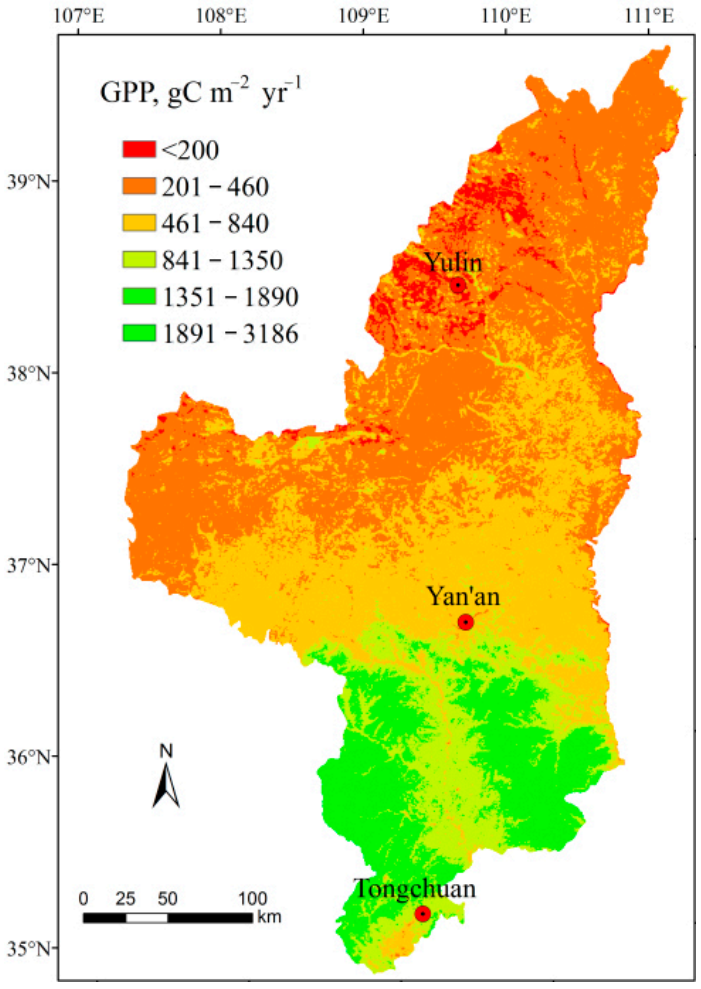

Figure 3. Spatial distribution of the mean GPP during 2000–2012 (g C m^{-2} yr^{-1}).

4.2. Temporal Variation and Trends of Annual GPP

During 2000–2012 (Figure 4), the annual mean GPP varied from 529.6 to 854.7 g C m^{-2} for the whole region and was 1231.6–1809.7, 953.1–1406.5, 390.8–712.4, and 428.8–701.4 g C m^{-2} for the forestland, shrubland, cropland, and grassland areas, respectively. This result indicates variation between years. The trend analyses indicate that variation in the re-

gion's mean GPP experienced a significant increasing trend. The variation increased by 11.7 g C m^{-2} yr^{-1} or 1.63% per year, but for the four land use areas, the change trend was different. In the cropland areas, the mean annual GPP showed a significant increasing trend at a 95% confidence level (Z = 2.26) with a rate of 2.62% per year, and in the grassland and shrub areas, a nonsignificant increasing trend (Z = 1.4 and Z = 1.1) was observed. In the forestland, no trend was detected (Z = 0.43) at a confidence level above 50%.

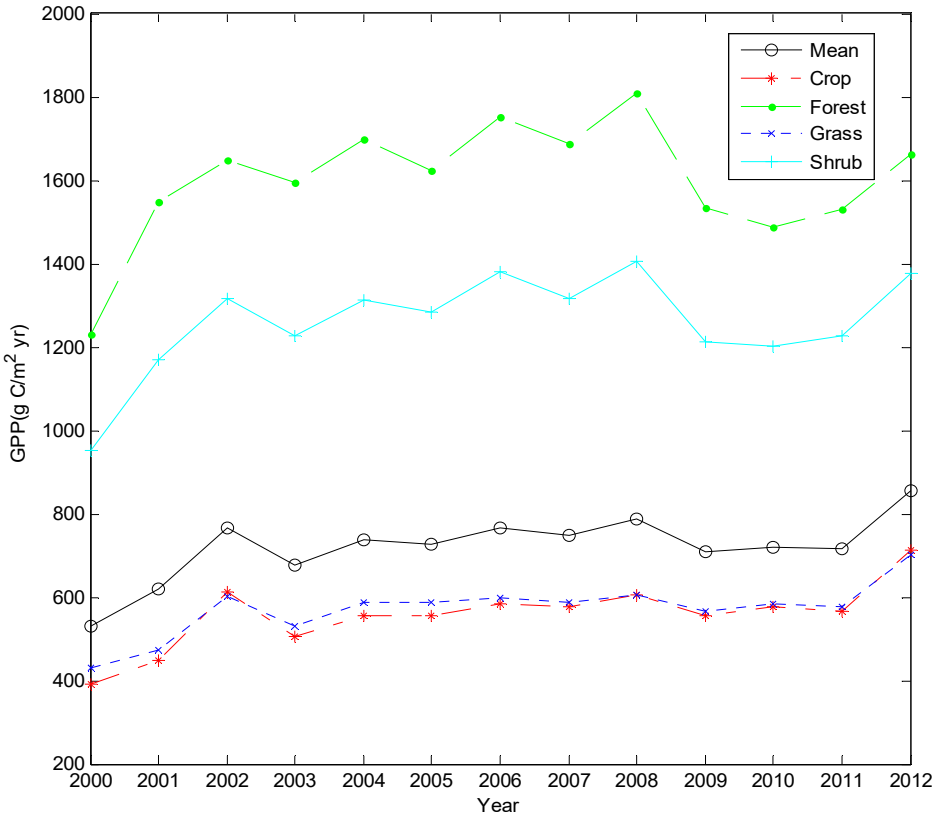

Figure 4. GPP variation of different vegetation and mean values (g C m^{-2} yr^{-1}).

Figure 5 presents the spatial distribution of annual GPP trends, categorized as follows: decreased significantly ($Z \leq -1.96$), decreased nonsignificantly (Z = −1.96 to −0.675), no trend ($|Z| < 0.675$), increased nonsignificantly (Z = 0.675 to 1.96), and increased significantly ($Z \geq 1.96$). It can be seen that the annual GPP experienced an increasing trend in the majority of the region. The statistical results indicate that in 80.2% of the pixels, the annual GPP presented an upward trend, while in a small area (1.8%), the annual GPP experienced a downward trend. Nearly half (47.8%) of the area showed a significant increasing trend at a 95% confidence level ($Z \geq 1.96$), which was mainly distributed in the gully areas of the middle and north areas (Figure 5), with the land use mainly including cropland in 2000 (Figure 2). The presence of change trends in annual GPP was not observed at above a 50% confidence level ($|Z| < 0.675$) in an area of 18.0%, which was mostly distributed in the southern forestland areas, dry northwestern, and northeastern grassland areas, where the dry climate is not suitable for forest vegetation.

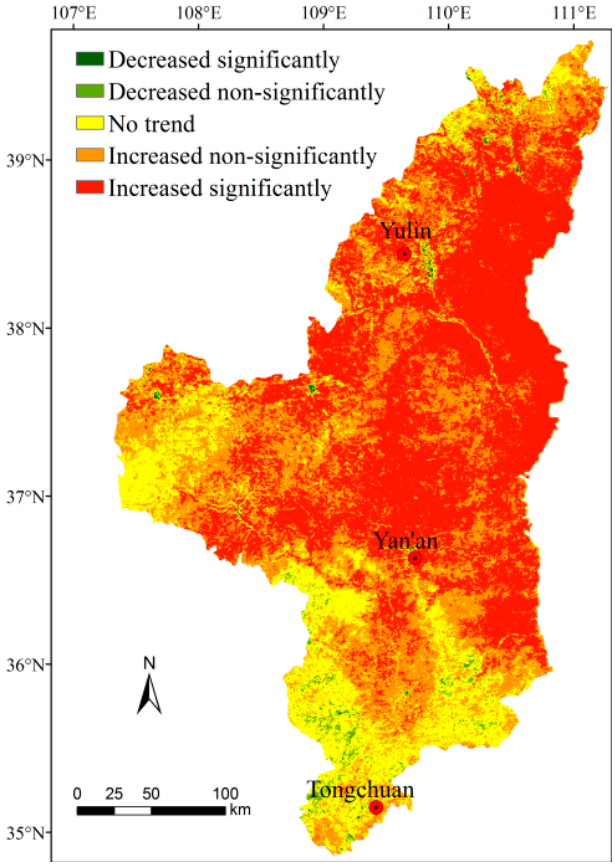

Figure 5. Spatial distribution of the change trend in annual GPP during 2000–2012.

4.3. Effects of Ecorestoration on GPP

At the county level, the mean annual GPP during 2000–2012 demonstrated a significant increasing trend for most of the 25 counties, with the mean annual change rate varying from 0.74 to 5.32%. During the same period, the mean annual afforestation rate was 0.90 to 3.71%. The regression analysis indicates that both values were significantly correlated (Figure 6).

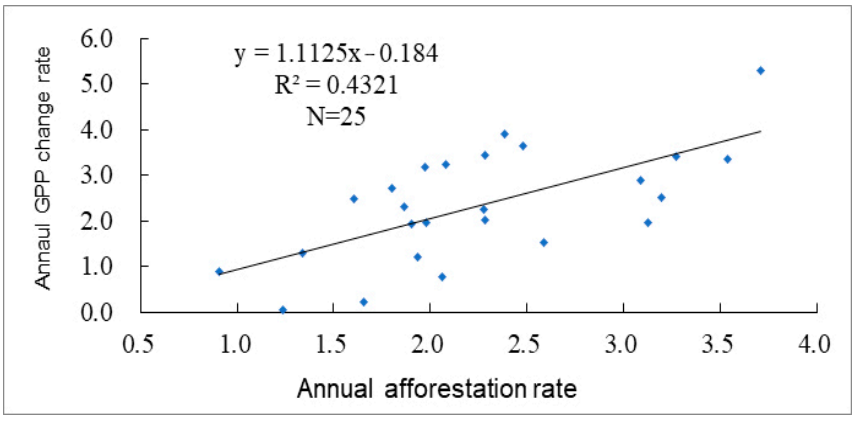

Figure 6. Relationship between annual change rates (%) in GPP and forestland (afforestation) rate (%).

In the typical area, the mean annual GPP increased significantly by 4.33% per year during 2000–2012 (Figure 7). For the two selected years, the mean annual GPP was 727.3 g C m^{-2} in 2009 and 526.6 g C m^{-2} in 2003, representing an increase of 38.4%. Meanwhile, the land use changed markedly, characterized by a great expansion of forestland and apparent shrinking of cropland and grassland (Table 1). The regression results using

the 117 fishnet data indicate that changes in GPP and forestland area were significantly correlated (Figure 8) with an R^2 of 0.6054. Multiple regressions including changes in other land use types, such as cropland, grassland, terraced areas, etc., did not indicate an evident increase in the correlation coefficient. This result suggests that these factors had a minor influence on the GPP increase.

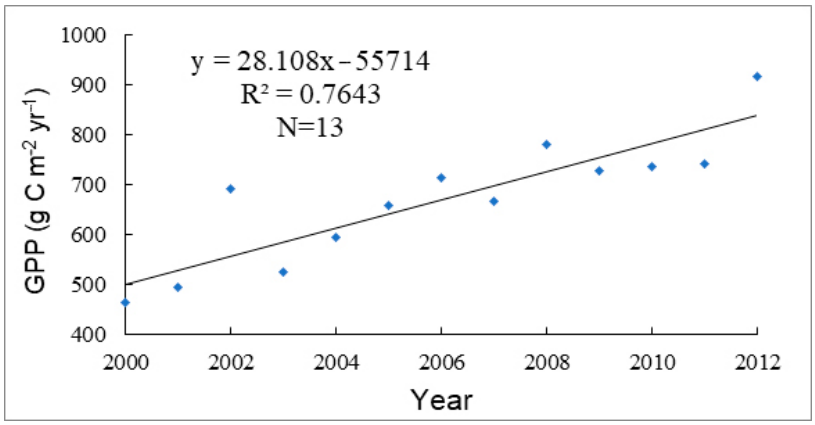

Figure 7. Trend in mean annual GPP in the typical area during 2000–2012.

Table 1. Area (ha) of major land use types in 2003 and 2009 and the changes in the typical area.

Land Use Type	2003	2009	Land Use Change	
			Area	%
Cropland	20,529.4	17,102.7	−3426.7	−16.7
Forestland	4812.2	11,369.4	6557.2	136.3
Grassland	54,054.2	50,079.0	−3975.2	−7.4
Shrubland	11,128.6	11,915.5	786.9	7.1

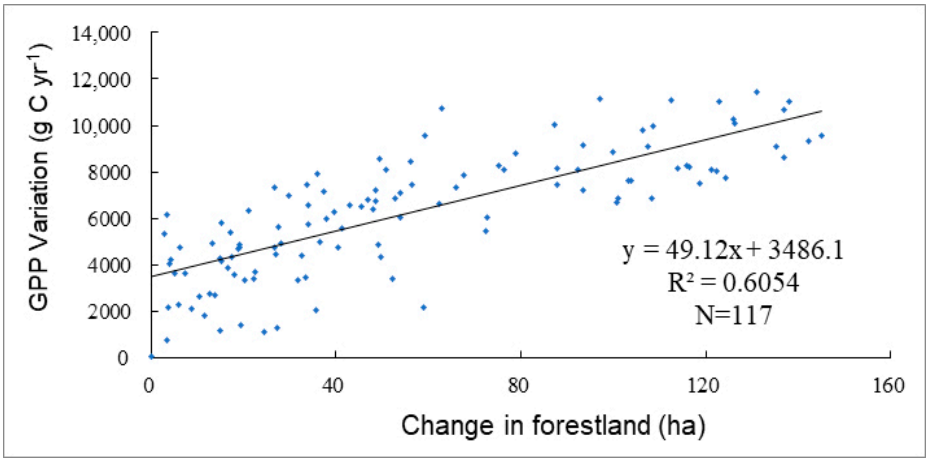

Figure 8. Relationship between changes in GPP and forestland area between 2003 and 2009 in the typical region.

Regarding the effects of climatic variation, the regression did not show a significant relationship between changes in GPP and the aridity index at the three representative sites. At the sites of Suide (cropland) and Yulin (grassland), the correlation coefficient R^2 was only 0.04, and at the site of Luochuan (forestland), it was 0.25.

5. Discussion

Except for the increase in forestland, the vegetation coverage in the region evidently improved during the period due to restricted grazing on grassland, improved cropland management, and strict protection of natural vegetation. We analyzed the change trend of the annual maximum EVI during 2000–2012 and found that in 90.4% of the region, the EVI or vegetation coverage experienced an increasing trend; for the whole region, this value increased by 1.47% per year. This finding is consistent with the results of several previous studies: Zhou et al. [42] found that the vegetation coverage in the same region significantly increased by 1.2% per year since the implementation of the GFG program. Chen et al. [43] indicated that from 1999 to 2013, vegetation coverage in the Loess Plateau almost doubled. In the Shaanxi–Gansu–Ningxia region, Li et al. [44] found that 97.4% of the region experienced an upward trend in vegetation coverage during 2000–2014 and concluded that the vegetation gradually stabilized. By analyzing the NPPs of different types of vegetation, Wang and Shangguan [45] observed that a change of vegetation was the most important factor affecting biomass change in the Loess Plateau.

It should be noted that the GPP was estimated using a simple light use efficiency model, and the results were not tested due to lack of available observational data. Compared to data from the limited literature in the similar areas, the estimated GPP seemed reasonable. For instance, the estimated grass GPP in 2008 was 606.6 g C m^{-2} yr^{-1}, which is close to the value of 616.8 g C m^{-2} yr^{-1} in a similar area reported by Wang et al. [38]. The mean GPP was 571.2 g C m^{-2} yr^{-1}, which is 16.2% lower than the value of 617.5 g C m^{-2} yr^{-1} [46]. The estimated forest GPP was 1594.8 g C m^{-2} yr^{-1} in 2003 and 1623.0 g C m^{-2} yr^{-1} in 2005—11.29% and 8.2% higher than the relevant records of 1433.0 and 1490.0 g C m^{-2} yr^{-1} [47], respectively.

Ultimately, this study analyzed the effect of the GFG program on primary plant production, thereby contributing to the understanding of the program's role in promoting restoration of the destroyed vegetation. The results suggest that the program has efficiently improved plant productivity and should continue to be supported by the government.

6. Conclusions

The study results indicate that the annual region's mean GPP varied from 529.6 to 854.7 g C m^{-2} during 2000–2012, with a 13-year average of 720 g C m^{-2}. The trend analyses indicate that in 80% of the region, the GPP experienced an increasing trend, and in nearly half of the region, the increasing trend was statistically significant. Spatial analysis showed that the GPP increased more significantly in the gully areas of the middle north, which was a key implementation area of the GFG program, while no evident trend was observed in the southern forestland areas. This result illustrates that the increase in GPP during 2000–2012 likely benefited primarily from the GFG program. We estimated from the regression results that the restoration of forest vegetation promoted by the GFG program could have contributed 40–60% to the increased GPP in the region. The remaining part could be attributed to the improvement in vegetation coverage due to vegetation protection and the growth of planted trees.

Author Contributions: W.L.: Methodology, data processing, formal analysis, resources, writing—original draft, and reviewing and editing. D.C.: Conceptualization and writing—reviewing and editing. All authors have read and agreed to the published version of the manuscript.

Funding: This work was supported by the Scientific Research Foundation of Suzhou University of Science and Technology (331812115), the National Natural Science Foundation of China, grant number 41971245, and the Fundamental Research Funds for National University, China univer-sity of Geosciences (Wuhan), grant number CUGDCJJ202223.

Institutional Review Board Statement: Not applicable.

Informed Consent Statement: Not applicable.

Data Availability Statement: The data presented in this study are available on request from the corresponding author.

Conflicts of Interest: The authors declare no conflict of interest.

References

1. Zhang, D.; Jia, Q.; Wang, P.; Zhang, J.; Hou, X.; Li, X.; Li, W. Analysis of spatial variability in factors contributing to vegetation restoration in Yan'an, China. *Ecol. Indic.* **2020**, *113*, 106278. [CrossRef]
2. Li, S.; Yan, J.; Liu, X.; Wan, J. Response of vegetation restoration to climate change and human activities in Shaanxi–Gansu–Ningxia Region. *J. Geogr. Sci.* **2013**, *23*, 98–112. [CrossRef]
3. Liu, J.; Li, Z.; Zhang, X.; Li, R.; Liu, X.; Zhang, H. Responses of vegetation cover to the Grain for Green Program and their driving forces in the Helongregion of the middle reaches of the Yellow River. *J. Arid. Land* **2013**, *5*, 511–520. [CrossRef]
4. Xu, Y.; Yang, B.; Tang, Q.; Liu, G.; Liu, P. Analysis of comprehensive benefits of transforming slope farmland to terraces on the Loess Plateau: A case study of the Yangou Watershed in Northern Shaanxi Province, China. *J. Mt. Sci.* **2011**, *8*, 448–457. [CrossRef]
5. Zhou, H.; Huang, S.; Wang, Y.; Wang, J.; Jia, H. Multi-scales Analysis of Driving Forces on Land Use_Cover Change in China: Taking Farmland Returning to Forest or Grassland as a Case. *Chinese J. Popul. Resour. Environ.* **2006**, *4*, 21–27. [CrossRef]
6. Wang, F.; Li, R.; Jiao, F.; Yang, Q.; Tian, J. The impact of cropland conversion on environmental effect in the Loess Plateau: A pilot study based on the national experimental bases. *J. Geogr. Sci.* **2005**, *15*, 484–490. [CrossRef]
7. Fu, B.; Liu, Y.; Lü, Y.; He, C.; Zeng, Y.; Wu, B. Assessing the soil erosion control service of ecosystems change in the Loess Plateau of China. *Ecol. Complex.* **2011**, *8*, 284–293. [CrossRef]
8. Chang, R.; Fu, B.; Liu, G.; Liu, S. Soil Carbon Sequestration Potential for "Grain for Green" Project in Loess Plateau, China. *Environ. Manag.* **2011**, *48*, 1158–1172. [CrossRef]
9. Chen, L.; Gong, J.; Fu, B.; Huang, Z.; Huang, Y.; Gui, L. Effect of land use conversion on soil organic carbon sequestration in the loess hilly area, loess plateau of China. *Ecol. Res.* **2007**, *22*, 641–648. [CrossRef]
10. Feng, Z.; Yang, Y.; Zhang, Y.; Zhang, P.; Li, Y. Grain for Green policy and its impacts on grain supply in west China. *Land Use Policy* **2005**, *22*, 301–312. [CrossRef]
11. Xu, Z.; Xu, J.; Deng, X.; Huang, J.; Uchida, E.; Rozelle, S. Grain for Green versus grain conflict between food security and conservation set-aside in China. *World Dev.* **2006**, *34*, 130–148. [CrossRef]
12. Xu, J.; Chen, L.; Lu, Y.; Fu, B. Sustainability Evaluation of the Grain for Green Project From Local People's Responses to Ecological Effectiveness in Wolong Nature Reserve. *Environ. Manag.* **2007**, *40*, 113–122. [CrossRef] [PubMed]
13. Yao, S.; Guo, Y.; Huo, X. An empirical analysis of effects of China's land conversion program on farmers' income growth and laber transfer. *Environ. Manag.* **2010**, *45*, 502–512. [CrossRef]
14. Xu, X.; Zhang, D.; Zhang, Y.; Yao, S.; Zhang, J. Evaluating the vegetation restoration potential achievement of ecological projects: A case study of Yan'an, China. *Land Use Policy* **2020**, *90*, 104293. [CrossRef]
15. Turner, D.P.; Ritts, W.D.; Zhao, M.; Kurc, S.A.; Dunn, A.L.; Wofsy, S.C.; Running, S.W. Assessing interannual variation in MODIS-based estimatof gross primary production. *IEEE Trans. Geosci. Remote Sens.* **2006**, *44*, 1899–1907. [CrossRef]
16. Jiang, Y.; Zhang, J.; Xua, X.; Dong, Z. A GPP assimilation model for the southeastern Tibetan Plateau based on CO2 eddy covariance flux tower and remote sensing data. *Int. J. Appl. Earth Obs. Geoinf.* **2013**, *23*, 213–225. [CrossRef]
17. Liu, J.F.; Chen, S.P.; Han, X.G. Modeling gross primary production of two steppes in Northern China using MODIS time series and climate data. *Procedia Environ. Sci.* **2012**, *13*, 742–754. [CrossRef]
18. Potter, C.S.; Randerson, J.T.; Field, C.B.; Matson, P.A.; Vitousek, P.M.; Mooney, H.A.; Klooster, S.A. Terrestrial ecosystem production: A process model based on global satellite and surface data. *Glob. Biogeochem. Cycles* **1993**, *7*, 811–841. [CrossRef]
19. Prince, S.D.; Goward, S.N. Global primary production: A remote sensing approach. *J. Biogeogr.* **1995**, *22*, 815–835. [CrossRef]
20. Veroustraete, F.; Sabbe, H.; Eerens, H. Estimation of carbon mass fluxes over Europe using the C-Fix model and Euroflux data. *Remote Sens. Environ.* **2002**, *83*, 376–399. [CrossRef]
21. Heinsch, F.A.; Reeves, M.; Votava, P.; Kang, S.; Milesi, C.; Zhao, M.; Glassy, J.; Jolly, W.M.; Loehman, R.; Bowker, C.F.; et al. User's Guide GPP and NPP (MOD17A2/A3) Products NASA MODIS Land Algorithm, Version 2.0. 2 December 2003. Available online: https://lpdaac.usgs.gov/documents/212/mod17_v5_user_guide.pdf (accessed on 24 May 2018).
22. Xiao, X.; Hollinger, D.; Aber, J.; Goltz, M.; Davidson, E.A.; Zhang, Q.; Moore, B., III. Satellite-based modeling of gross primary production in an evergreen needleleaf forest. *Remote Sens. Environ.* **2004**, *89*, 519–534. [CrossRef]
23. Yuan, W.; Liu, S.; Zhou, G.; Zhou, G.; Tieszen, L.L.; Baldocchi, D.; Bernhofer, C.; Gholz, H.; Goldstein, A.H.; Goulden, M.L.; et al. Deriving a light-use efficiency model from eddy covariance flux data for predicting daily gross primary production across biomes. *Agric. For. Meteorol.* **2007**, *143*, 189–207. [CrossRef]
24. Sims, D.A.; Rahman, A.F.; Cordova, V.D.; El-Masri, B.Z.; Baldocchi, D.D.; Bolstad, P.V.; Flanagan, L.B.; Goldstein, A.H.; Hollinger, D.Y.; Misson, L.; et al. A new model of gross primary productivity for North American ecosystems based solely on the enhanced vegetation index and land surface temperature from MODIS. *Remote Sens. Environ.* **2008**, *112*, 1633–1646. [CrossRef]
25. Wu, L.; Gu, S.; Zhao, L.; Xu, S.; Zhou, H.; Feng, C.; Xu, W.; Li, Y.; Zhao, X.; Tang, Y. Variation in net CO_2 exchange, gross primary production and its affecting factors in the planted pasture ecosystem in Sanjiangyuan Region of the Qinghai-Tibetan Plateau of China. *Chin. J. Plant Ecol.* **2010**, *34*, 770–780. [CrossRef]
26. Fensholt, R.; Sandholt, I.; Rasmussen, M.S. Evaluation of MODIS LAI, fAPAR and the relation between fAPAR and NDVI in a semi-arid environment using in situ measurements. *Remote Sens. Environ.* **2004**, *91*, 490–507. [CrossRef]

27. Turner, D.P.; Ritts, W.D.; Cohen, W.B.; Maeirsperger, T.K.; Gower, S.T.; Kirschbaum, A.A.; Running, S.W.; Zhao, M.; Wofsy, S.C.; Dunn, A.L. Others Site-level evaluation of satellite-based global terrestrial gross primary production and net primary production monitoring. *Glob. Chang. Biol.* **2005**, *11*, 666–684. [CrossRef]
28. Xiao, X.; Boles, S.; Liu, J.; Zhuang, D.; Liu, M. Characterization of forest types in Northeastern China, using multi-temporal SPOT-4 VEGETATION sensor data. *Remote Sens. Environ.* **2002**, *82*, 335–348. [CrossRef]
29. Xiao, X.; Zhang, Q.; Braswell, B.; Urbanski, S.; Boles, S.; Wofsy, S.; Moore, B., III; Ojima, D. Modeling gross primary production of temperate deciduous broadleaf forest using satellite images and climate data. *Remote Sens. Environ.* **2004**, *91*, 256–270. [CrossRef]
30. Xiao, X.; Zhang, Q.; Hollinger, D.; Aber, J.; Moore, B., III. Modeling gross primary production of an evergreen needleleaf forest using MODIS and climate data. *Ecol. Appl.* **2005**, *15*, 954–969. [CrossRef]
31. Li, W.J.; Lu, C.H. Aridity trend and response to vegetation restoration in the loess hilly region of northern Shaanxi Province. *J. Geogr. Sci.* **2015**, *25*, 289–300. [CrossRef]
32. Huete, A.R.; Liu, H.Q.; Batchily, K.; van Leeuwen, W. A comparison of vegetation indices over a global set of TM images for EOS-MODIS. *Remote Sens. Environ.* **1997**, *59*, 440–451. [CrossRef]
33. Angstrom, A. Solar and terrestrial radiation. Report to the international commission for solar research on actinometric investigations of solar and atmospheric radiation. *Q. J. R. Meteorol. Soc.* **1924**, *50*, 121–126. [CrossRef]
34. Zotarelli, L.; Dukes, M.D.; Romero, C.C.; Migliaccio, K.W.; Morgan, K.T. AE459 Step by Step Calculation of the Penman-Monteith Evapotranspiration (FAO-56 Method). Published by the UF Department of Agricultural and Biological Engineering. 2010. Available online: https://edis.ifas.ufl.edu/pdf/AE/AE45900.pdf (accessed on 20 May 2016).
35. Li, J.; Shao, M.; Zhang, X. Data base construction for the EPIC model on the Loess Plateau region. *J. Northwest AF Univ.* **2004**, *32*, 21–26. (In Chinese) [CrossRef]
36. Dennis, G.D. Spectral composition and quanta-to-energy ratio of diffuse photosynthetically active radiation under diverse cloud conditions. *J. Geophys. Res. Atmos.* **2004**, *109*, 159–173. [CrossRef]
37. 1:1 Million Vegetation Data Set in China. The Dataset is Provided by National Cryosphere Desert Data Center. Available online: http://www.ncdc.ac.cn (accessed on 6 July 2020).
38. Wang, H.; Jia, G.; Fu, C.; Feng, J.; Zhao, T.; Ma, Z. Deriving maximal light-use efficiency from coordinated flux measurements and satellite data for regional gross primary production modeling. *Remote Sens. Environ.* **2010**, *114*, 2248–2258. [CrossRef]
39. Sicard, P.; Mangin, A.; Hebel, P.; Malléa, P. Detection and estimation trends linked to air quality and mortality on French Riviera over the 1990–2005 period. *Sci. Total Environ.* **2010**, *408*, 1943–1950. [CrossRef]
40. Sen, P.K. Estimates of the regression coefficient based on Kendall's Tau. *J. Am. Stat. Assoc.* **1968**, *63*, 1379–1389. [CrossRef]
41. Salmi, T.; Määttä, A.; Anttila, P.; Ruoho-Airola, T.; Amnell, T. *Detecting Trends of Annual Values of Atmospheric Pollutants by the Mann-Kendall Test and Sen's Slope Estimates the Excel Template Application MAKESENS*; Finnish Meteorological Institute: Helsinki, Finland, 2002; Volume 31.
42. Zhou, H.; Van Rompaey, A.; Wang, J. Detecting the impact of the "Grain for Green" program on the mean annual vegetation cover in the Shaanxi province, China using SPOT-VGT NDVI data. *Land Use Policy* **2009**, *26*, 954–960. [CrossRef]
43. Chen, Y.; Wang, K.; Lin, Y.; Shi, W.; Song, Y.; He, X. Balancing green and grain trade. *Nat. Geosci.* **2015**, *8*, 739–741. [CrossRef]
44. Li, S.; Yang, S.; Liu, X.; Liu, Y.; Shi, M. NDVI-Based Analysis on the Influence of Climate Change and Human Activities on Vegetation Restoration in the Shaanxi–Gansu–Ningxia Region, Central China. *Remote Sens.* **2015**, *7*, 11163–11182. [CrossRef]
45. Wang, K.; Shangguan, Z. Simulating the vegetation-producing process in small watersheds in the Loess Plateau of China. *J. Arid. Land* **2012**, *4*, 300–309. [CrossRef]
46. Zhang, F.; Zhou, G.; Wang, Y. Dynamics simulation of net primary productivity by a satellite data-driven CASA model in Inner Mongolian typical steppe, China. *J. Plant Ecol.* **2008**, *32*, 786–797. [CrossRef]
47. Wu, J.; Xiao, X.; Guan, D.; Shi, T.; Jin, C.; Han, S. Estimation of the gross primary production of an old growth temperate mixed forest using eddy covariance and remote sensing. *Int. J. Remote Sens.* **2009**, *30*, 463–479. [CrossRef]